Chemistry
A European
Journal

Chemistry Europe
European Chemical Societies Publishing

Accepted Article

Title: Synthesis and optimization of zeolitic imidazolate frameworks for oxygen evolution reaction

Authors: Juntao Li and Srinivas Gadipelli

To be cited as: *Chem. Eur. J.* 10.1002/chem.202002702

Link to VoR: https://doi.org/10.1002/chem.202002702

WILEY-VCH

10.1002/chem.202002702

WILEY-VCH

Synthesis and optimization of zeolitic imidazolate frameworks for oxygen evolution reaction

Juntao Li,*[a] and Srinivas Gadipelli*[a,b,c]

[a] J. Li, Dr. S. Gadipelli.
Department of Chemistry
University College London
London, WC1H 0AJ, United Kingdom
E-mail: juntao.li.16@ucl.ac.uk; s.gadipelli@ucl.ac.uk
[b] Dr. S. Gadipelli
Department of Chemical Engineering
University College London
London, WC1E 7JE, United Kingdom
[c] Dr. S. Gadipelli
College of Physics
Sichuan University
Chengdu, 610064, China
Email: s.gadipelli@scu.edu.cn

Abstract: Metal-organic frameworks/Zeolitic imidazolate frameworks (MOFs/ZIFs) and their post-synthesis modified nanostructures, such as oxides, hydroxides and carbons have generated significant interest for electrocatalytic reactions. In this work, we report a high and durable oxygen evolution reaction (OER) performance from bimetallic $Zn_{100-x}Co_x$-ZIF samples directly, without carrying out high-temperature calcination and/or carbonization. ZIFs can be reproducibly and readily synthesized in large scale at ambient conditions. The bimetallic ZIFs show a systematic and gradually improved OER activity with increasing cobalt concentration. A further increase in OER activity is evidenced in ZIF-67 polyhedrons with controlled particle size of <200 nm among samples of different sizes between 50 nm and 2 µm. Building on this, a significantly enhanced, >50%, OER activity is obtained in ZIF-67/carbon black, which shows a low-overpotential of ~320 mV in 1.0 M KOH electrolyte. Such activity is comparable or better to numerous MOFs/ZIFs derived electrocatalysts. The optimized ZIF-67 sample also exhibits increased activity and durability over 24 h, which is attributed to in-situ developed active cobalt-oxide/oxyhydroxide related nanophase.

Introduction

Metal-organic frameworks (MOFs) and their derived nanostructures have opened up phenomenal interest for numerous applications, such as molecular uptake, separation and catalysis (both heterogeneous and electrochemical).[1-7] For example, the MOFs derived nanostructures, often in the forms of nanosheets, oxides, hydroxides/oxyhydroxides and metal/metal-oxide embedded carbons, obtained via high temperature thermolysis route, have shown a great promise for electrocatalysis reactions, such as oxygen reduction, oxygen evolution and hydrogen evolution reactions (ORR, OER and HER, respectively).[8-14] Here, it is worth noting that thermolysis process of MOFs involve severe decomposition of the organic ligand and mass-loss.[2,6,15] For instance, as low as (10–20) wt% of porous carbon is produced from MOF-5 or MOF-74 (Zn).[16] In order to utilize MOFs more efficiently and to avoid issues related to reproducibility (in terms of controlling the composition, functionality, heterogeneity, porosity and nanophase) and mass production, it is highly desirable to avoid extensive modification of MOFs. For these reasons, the recent works have focussed on mild post-synthesis modification or even direct utilization of MOFs/ZIFs.[10,12,15,17-19]

In principle, MOFs with open framework structure composed of metal nodes and ligand heterofunctional groups are ideal candidates for electrocatalytic reactions, which proceed via adsorption/conversion of gaseous/liquid phase reactants and products at a triple phase boundary of solid-liquid-gas interface involving catalyst-electrolyte-oxygen.[4,20-25] MOFs can offer favorable adsorption/catalytic activities with the intrinsically rich surface functional groups, adsorption/catalytic sites, accessible pore channels as well as high specific surface area and topological structure. Moreover, MOFs can be readily functionalized with metal ions to produce mixed-metal MOFs.[13,17,20,26] Bimetallic MOFs are attractive owing to the advantages of widely tunable reactive surface/interface chemistry/composition along with external nano/microstructure in different dimensionality, which in turn can offer extensive surface adsorption, binding, catalytic site density and electron/mass transport. For instance, rationally designed bimetallic MOFs have resulted in enhanced structural stability and OER performance compared to the monometallic MOFs.[13,17,20,26–28] A highly improved hydrolytic stability and heterogeneous catalytic activity is reported in Zn/Co-ZIF-8 compared to ZIF-8 and ZIF-67.[20,28] In addition to this, bimetallic layered double hydroxide based nanowire arrays with ZIF-67 flower-like structures and cobalt-oxides/hydroxides are also designed to extract OER activity with respect to ZIF-67.[10,11,29] It is also reported that the incorporation of second metal cation, catalytically inactive Zn^{2+} in CoOOH derived from ZIF-67 deliver a highly improved activity and stability for OER.[30] A significantly enhanced OER performance is observed in $Zn_xCo_{3-x}O_4$ nanostructures over Co_3O_4 alone.[31] Furthermore, Co/Zn atomic dual-sites anchored on N-doped carbon nanofibers in $N_2CoN_2ZnN_2$ configuration delivered greatly enhanced ORR activity and stability compared to Co or Zn mono-sites samples in the traditional $Co–N_4$ or $Zn–N_4$ configuration.[32]

Considering the advantages of bimetal based catalysts, in this work, we select bimetallic MOFs based system, $Zn_{100-x}Co_x$-ZIF-8 to explore OER catalytic activity with respect to the composition and particle size, in the as-synthesized samples. Furthermore, ZIF-8 is commercially available MOF, and ZIF-8 or its isostructural analogue ZIF-67 can be readily synthesized in a large scale under mild conditions or at room temperature and ambient pressure using commonly used laboratory washing solvents (e.g. methanol), by stirring, microwave and continuous flow or solid-state routes.[33,34] The prototype ZIF-8 exhibits high accessible surface area for many gaseous and liquid molecules.[19,35,36] Furthermore, ZIF-8/ZIF-67 formed by imidazolate linkers and a single-metal-atom (Zn or Co)–N_4 tetrahedron, is reminiscent to the proposed active M-N_4 (M = Mn, Fe, Co, etc.) sites in carbonaceous electrocatalysts.[1–4,7,33] Therefore, a new strategy to extract the electrocatalytic activity from as-received bimetallic $Zn_{100-x}Co_x$-ZIFs is developed. The electrochemical tests show that OER activity of ZIF-8(Zn) is gradually enhanced towards ZIF-67(Co) with the substitution of cobalt metal for zinc. Further to this, ZIF-67 crystallites of varied sizes, between 50 nm to 2000 nm, are examined to achieve the best catalytic performance. A well-correlated activity relationship with respect to the particle-size is evidenced, in which increase in particle size leads to reduced activity. Building upon this understanding, a highly enhanced OER activity is obtained from ZIF-67/carbon black composite (ZIF-67/CB). This performance is comparable or even superior to many literature reports of MOFs/ZIFs based carbonaceous nanostructures. The ZIF-67/CB samples also show growing evidence for oxygen reduction reaction (ORR) activity to function as dual activity for both OER and ORR. These optimized ZIF-67 samples also exhibit stable OER activity durability for several hours. Interestingly, ZIF-67 nanoparticles coated on the carbon paper show highly increased activity stability over 24 h in 1 M KOH electrolyte. The samples characterised after OER durability test indicate a decomposition of ZIF-67 structure to active cobalt-oxide/oxyhydroxide related active phase.

Results and Discussion

ZIF-8 and ZIF-67 samples are synthesized by stirring at room temperature from methanolic solutions of precursors, according to previous reports.[37] The as-formed ZIFs are then thoroughly characterized and used for catalytic studies without high-temperature outgassing or activation. All the sample handling is carried out under ambient atmosphere. Characterizations, such as powder X-ray diffraction (PXRD), Fourier-transform infrared (FTIR) spectroscopy, X-ray photoemission spectroscopy (XPS), scanning and transmission electron microscopy (SEM and TEM) and gas adsorption/porosity isotherms show a well-developed framework structure and isostructural nature of samples (Figure 1, and Figure S1-S3; Table S1).[19,37] SEM and TEM micrograph shows well-defined crystallite facets of rhombic dodecahedral nanocrystals of uniform sizes (Figure 1d and Figure S2). N_2 adsorption isotherms yield high specific surface area of ~1700 $m^2\ g^{-1}$ and porosity of 0.7 $cm^3\ g^{-1}$ in the samples (Figure 1e, S3, Table S1). The similar structural features, porosity and CO_2 uptake inform the quality of the samples (Figure S4).[37] As shown in Figure 1f, the initial electrochemical catalytic

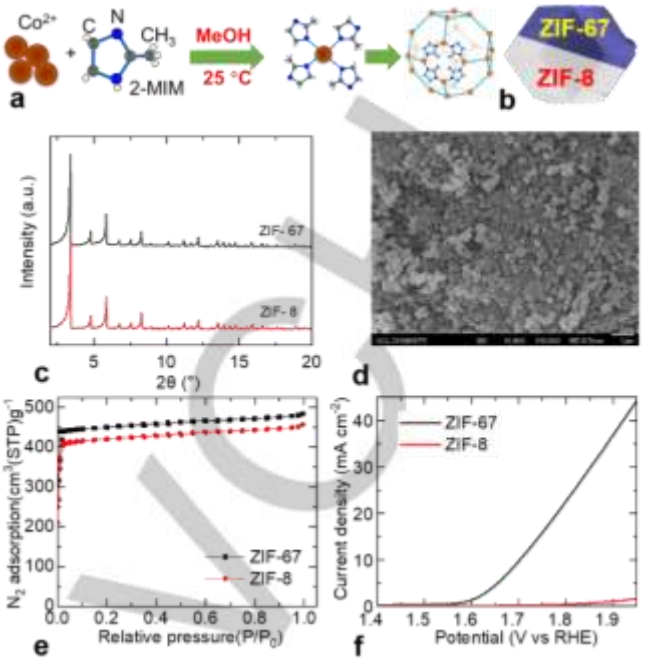

Figure 1. Structural and OER characteristics of ZIF-8 and ZIF-67: a-b) Illustration of formation of ZIF-67 structure with a Co–N_4 coordination and a SEM image of ZIF-8/ZIF-67 crystal. **c)** PXRD patterns (a.u. = arbitrary units). **d)** SEM image of ZIF-67 with average particle size of 200 nm. **e)** Nitrogen adsorption-desorption isotherms. **f)** OER LSV curves in 0.1 M KOH electrolyte.

assessment of samples by linear sweep voltammetry (LSV) shows surprising OER activity difference between ZIF-8 and ZIF-67. The ZIF-8 exhibits a negligible OER activity compared to a high current response from ZIF-67. A potential of ~1.72 V (vs RHE with onset potential being close to 1.6 V) to reach an impressive benchmark current density of 10 mA cm^{-2} in ZIF-67 is comparable to many of the carbon based nanostructures.[35,37–39]

In order to explore the OER activity evolution from ZIF-8 to ZIF-67, a series of bimetallic $Zn_{100-x}Co_x$-ZIF-8 samples of controlled particle size is rationally designed with gradual replacement of zinc by cobalt (Figure 2, S5-S8 and Table S1, S2). PXRD patterns, FTIR and XPS spectra, SEM/TEM images and N_2 adsorption isotherms indicate that all the samples are isostructural in nature with high crystallinity, framework and porosity as the parent ZIF-8 structure.[4,37] Here, it is worth noting a slight changes for peaks in XPS (Zn 2p and Co 2p) and FTIR (M-N vibrational mode at ~420 cm^{-1}) spectra with respect to the composition (Figure S5, S6). Thermogravimetry curves demonstrate a clear change in their thermal stability and residual mass with an increase of the cobalt substitution for the zinc (Figure S8). It is interesting to note that the LSV curves reveal a continuously enhanced OER activity when going from zinc based ZIF-8 to cobalt based ZIF-67 (Figure 2g). Though the combination of metal centres or bimetallic ZIFs does not offer any synergistic effect for improved OER activity, it confirms that most of their activity can be attributed directly to the cobalt metal centres.[27]

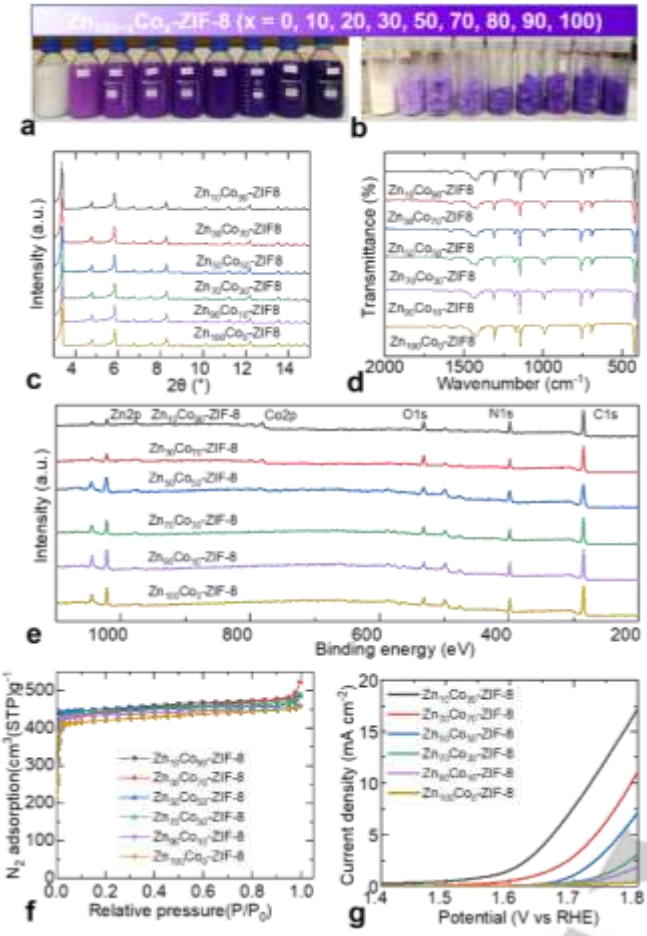

Figure 2. Structural characteristics and OER activities of bimetallic ZIFs, $Zn_{100-x}Co_x$-ZIF-8: a-b) Photographs of respective reaction solvents in glass jars and powdery samples in vials – a total methanol precursors solvent of 1 litre volume in each case is used to obtain a sample of over a gram quantity. **c)** PXRD patterns (a.u. = arbitrary units). **d)** FTIR spectra. **e)** XPS survey spectra. **f)** Nitrogen adsorption-desorption isotherms. **g)** OER LSV curves, obtained in 0.1 M KOH electrolyte.

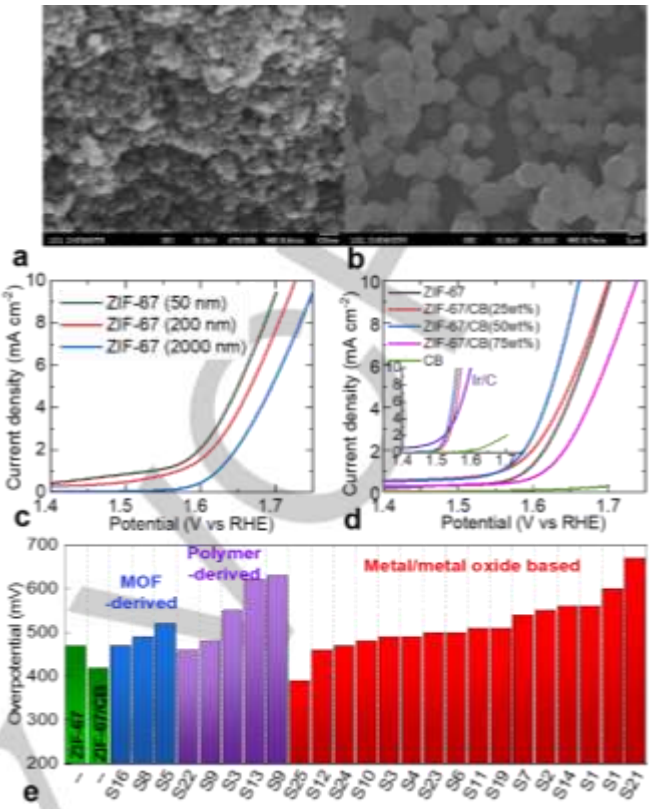

Figure 3. Optimised ZIF-67 and OER activity: a-b) SEM images of samples with controlled particle sizes of 50 nm and 2000 nm. **c)** LSV curves of ZIF-67 samples with different particle sizes, measured in 0.1 M KOH. **d)** LSV curves of ZIF-67/CB samples with varied amount of CB, measured in 0.1 M KOH and 1.0 M KOH (inset). Reference Ir/C data is reproduced from [9]. **e)** Overpotential values, estimated at the current density of 10 mA cm^{-2} in a 0.1 KOH electrolyte, for the ZIF-67(50 nm), ZIF-67/CB (50 wt%) and carbon based catalysts from the published literature. Smaller overpotential value is an indicator for best OER catalyst and different colour indicate different precursor. Detailed activity values and sample identities are summarised in Table S3.

Next, ZIF-67 samples of different particle sizes between 50 nm to 2000 nm are synthesized to achieve best catalytic activity performance (Figure 3a,b, S9, S10 and Table S1). Interestingly, a well-correlated performance relationship with respect to the particle-size of ZIFs is evidenced (Figure 3c). A further improved OER activity is observed in the sample with particle size of ~50 nm (ZIF-67(50 nm)). The overpotential required to reach a current density of 10 mA cm^{-2} is now 480 mV, about 20 mV and 50 mV lower than the samples with particle size of 200 nm and 2000 nm respectively. As this catalytic reaction process involves solid-liquid surface-interface associated adsorption, dissociation, intermediates, migration and charge transport to the electrode collector, the smaller crystals with more active surface area are expected to show a favourable performance.[7] Here, it is worth noting that all the samples are in isostructural nature and exhibit identical frameworks structure and porosity, thus the activity difference is directly attributed to their particle-size (Figure 3, S9 and Table S1). ZIF-67(50 nm) also exhibits smaller Tafel slope 84.4 mV dec^{-1} (Figure S10). The improved OER activity in ZIF-67(50 nm) can also be attributed to its excess mesoporosity formed by external surfaces from the nanoparticle assembly.

The above results and literature further suggest that catalytic activity of ZIF-67 nanoparticles can be enhanced by increasing the electrical conductivity.[9–11] Hence, a set of ZIF-67/CB samples with varying amounts of CB (at 25 wt%, 50 wt% and 75 wt%) are prepared by simple physical mixing. A noteworthy improvement in the OER performance is seen for ZIF-67/CB (50 wt%) (Figure 3d). Specifically, both onset and potential at 10 mA cm^{-2} is reduced. The CB alone does not show any OER activity. As shown in Figures S11 and S12, this improved OER activity in ZIF-67/CB (50 wt%) sample is attributed to enhanced electrochemical surface area and smaller Tafel slope. Here it is worth noting that this OER activity is comparable or better than the many carbon based nanostructures include MOFs and ZIFs-derived metal-incorporated carbons produced by extensive chemical treatment (Figure 3e).[27,35,37–40] For example, the OER performance of ZIF-67 and other carbon nanostructures produced at elevated temperatures, between 700-1100 °C from the inorganic, MOF, polymeric, graphene-oxide precursors and templates, and in their heteroatom doping and metal-/metal-oxide grafting states, as summarized in Table S3. The OER activity is also higher than the commercial Pt/C, and approaching the benchmark material, IrO_2/C (Figure 3e).[27] An enhanced OER activity of these ZIF-67/CB samples is also

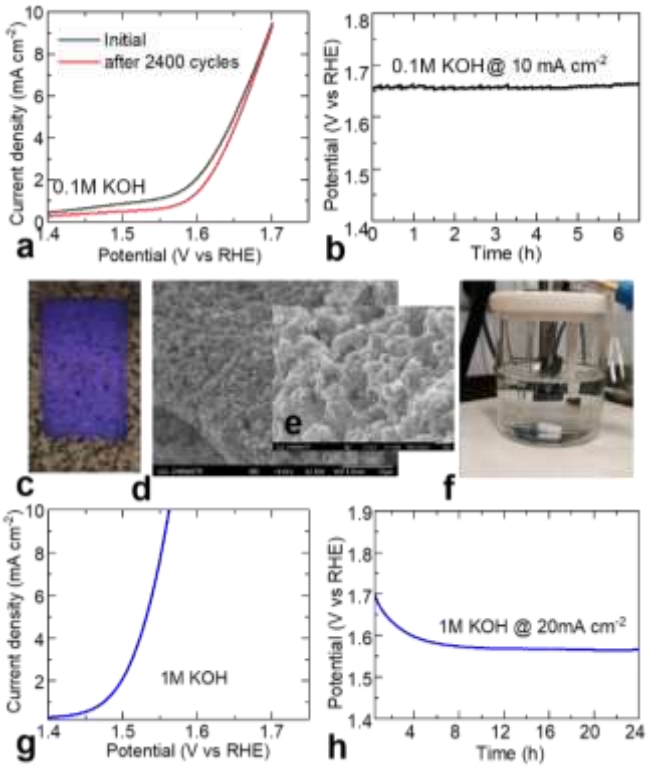

Figure 4: OER activity durability of optimised ZIF-67 sample: a) Comparative LSV curves of ZIF-67 before and after 2400 CV tests. **b)** Chronopotentiometry of ZIF-67 at a current density of 10 mA cm^{-2} and 1600 rpm. In (a-b) the ZIF-67 is depositd on GCE, measured for 6 h in 0.1 M KOH. **c-f)** Photograph, SEM micrographs of before (d) and after (e) OER stability and 3-electrode test cell for ZIF-67 sample deposited on carbon paper with a loading of 2 mg cm^{-2}. **g)** LSV curve ZIF-67 sample deposited on carbon paper, measured in 1 M KOH. **h)** Chronopotentiometry of ZIF-67 sample deposited on carbon paper, measured for 24 h in 1 M KOH, at a current density of 20 mA cm^{-2}.

observed in the 1.0 M KOH electrolyte (inset of Figure 3d and Figure S13). Now the overpotential is reduced to about 320 mV to deliver 10 mA cm^{-2}, which is better or comparable to many of the modified ZIF-67 based hybrid nanostructures of nanosheets, oxides, hydroxides, and carbon based heterostructures as well as reference Ir/C (300-343 mV).[8–11,13,15,17,26,41] In addition, it is very interesting to see an emerging oxygen reduction reaction (ORR) activity in the ZIF-67/CB samples (Figure S14). Though no ORR activity is observed for both ZIF-67 and CB alone, a continuously improved activity, with prominent current response at further reduced potentials, can be seen for ZIF-67/CB samples with respect to the increased amount of CB. Such activity is also evidenced in CV curves with a characteristic cathodic current peak. These observations clearly suggest that the dual activity for both OER and ORR can be extracted from ZIF-67 with a suitable conducting matrix.

The other important parameter, OER durability/stability of the ZIF-67 is investigated by three different methods: chronoamperometry (*i vs t*), chronopotentiometry (*V vs t*) and accelerated CV scans at 100 mV s^{-1} (Figure 4, S15). The sample shows an impressive durability over several hours of continuous operation. Here it is worth noting that OER stability of ZIF-67 is superior to the many carbonaceous structures. For instance, after 2400 CV cycles, of continuous operation over ~6 hours, ZIF-67 sample shows negligible drop in activity (Figure 4a). The *V vs t* and *i vs t* data also shows a similar durability (Figure 4b, S15). The data presented in Figures 4a,b and S13 is recorded for the samples coated onto a glassy carbon electrode (GCE) and measured under constant rotation of 1600 rpm in 0.1 M KOH. A partial activity decay in stability tests may be attributed to gradual loss of catalyst on the electrode under rotation.[35,37,39] Catalyst detachment from GCE surface is often observed. Therefore, further to alleviate this problem and to understand the true activity durability performance, $Zn_{100-x}Co_x$-ZIF-8 samples are deposited on to a carbon paper (with a high mass loading of 2.0 mg cm^{-2}). Figure 4c-f shows photographs of ZIF-67/carbon paper and 3-electrode test cell, as well as SEM micrographs. The LSV data recorded in 1.0 M KOH electrolyte while stirring solution with a bar magnet shows a similar performance to the RDE data obtained for ZIF-67/CB(50wt%) sample (Figure 4g). More importantly, it not only shows a high durability but also exhibits further improved performance over the time, which increases exponentially for few hours and then stabilizes during 24 h continuous test (Figure 4h). This trend is also observed in $Zn_{100-x}Co_x$-ZIF-8 samples (Figure S16) and can be attributed to increased electrolyte accessibility to hydrophobic ZIF-67 structure over the time. FTIR, SEM, XPS and PXRD characterizations of $Zn_{100-x}Co_x$ZIF-8 samples after OER durability tests reveal transformation of ZIFs to active cobalt based oxide/oxyhydroxide nanophase, in a good agreement with the literature reports (Figures S17 to S20).[9-11,17,42–44] As shown in Figure S17, the FTIR spectra show development of new Co–O vibrational mode (at 523 cm^{-1}) at the expense of Zn/Co-N coordination (at 420 cm^{-1}) in $Zn_{100-x}Co_x$ZIF-8 samples. Similarly, XPS spectra of Co 2p in a parent ZIF-67 sample with two peaks at around 782 eV and 797.7 eV shift to lower binding energy without satellite peaks in the sample used for OER test for 24 h, supporting the formation of cobalt oxide/hydroxide phase (Figure S18).[44–46] XRD profiles and SEM images further indicates the transformation of crystalline ZIF-67 to amorphous phase (Figure S19), in a good agreement with earlier reports of MOFs/ZIFs based OER catalysts (Figure S20).[44,47] Overall, such results suggest that ZIF-67 is a promising and inexpensive catalyst, and its activity for OER or ORR or both can be further improved by tailoring framework/mico/nano structure by the strategic design of MOFs/ZIFs.[9,10,13,26]

Conclusion

We have disclosed a highly active and durable OER performance, for the first time, in one of the widely studied MOF structures, ZIF-67 – a cobalt based prototype of ZIF-8 directly, without carrying any further post-synthesis chemical modification such as oxidation or carbonization at high temperature. Co–N, rather than Zn–N, coordination is responsible for the oxygen catalysis reactions, which is identified by screening a series of bimetallic $Zn_{100-x}Co_x$-ZIF-8 samples with a progressive cobalt substitution for zinc metal centres. Such activity is further enhanced in the optimized ZIF-67 with control over particle size as well as with conducting support. Interesting correlation is observed between OER and particle size of ZIF-67, where the samples of particle size 50 nm and 2000 nm exhibit an overpotential difference of about 50 mV at 10 mA cm^{-2} with a decreased activity trend against increased particle size. Such activities are further improved by the addition of conducting

carbon black or depositing on carbon paper, with a low overpotential of ≈320 mV to achieve a current density of 10 mA cm^{-2} in 1.0 M KOH electrolyte. Samples also exhibit highly durable OER activity over several hours of continuous tests. The OER activity in optimized ZIF-67 nanoparticles is comparable to the carbonaceous nanostructures, include MOFs/ZIFs derived carbons. The catalyst samples probed after OER durability tests indicate in-situ development of active amorphous nanophase of cobalt-oxide/oxyhydroxide. The present study provides a straightforward and energy-efficient strategy for designing electrocatalysts and suggests further improved activities in the tailoring framework structures in terms of dimensionality, pore geometry, and accessible surface with combined macro-micropore channels and hydrophilicity.

Experimental Section

ZIF-8, ZIF-67 and bimetallic $Zn_{100-x}Co_x$-ZIF-8 samples were synthesized in a similar method according to the reported procedure.[37] Briefly, for ZIF-8 (or ZIF-67), 7.344 g of zinc nitrate hexahydrate (or cobalt nitrate hexahydrate) was dissolved in 500 ml methanol. Then, 8.106 g of 2-methyl imidazole was mixed in another 500 ml of methanol with ~4 ml 1-methylimidazole. Then the solution was stirred and slowly added to the metal precursor solution. After a few minutes, the solution changed from the clear (or pink for cobalt) to milky white (or purple for cobalt), which was then left for a day to settle. A clear solution was poured out and the precipitate sample was extracted after several washings with methanol. All the samples were dried at 80 °C oven. The bimetallic $Zn_{100-x}Co_x$-ZIF-8 samples were synthesized in a similar method but by replacing the portion of the zinc nitrate precursor with cobalt nitrate. For example, the sample made with 10%, 20% and 50% by mass of the cobalt nitrate replacing the zinc nitrate (more precisely, for 10%: 0.7344 g of cobalt nitrate + 6.6096 g of zinc nitrate; for 20%: 1.479 g of cobalt nitrate + 5.875 g of zinc nitrate; for 50%: 3.672 g of cobalt nitrate + 3.672 g of zinc nitrate) are named as $Zn_{90}Co_{10}$-ZIF-8, $Zn_{80}Co_{20}$-ZIF-8 and $Zn_{50}Co_{50}$-ZIF-8 respectively.

Synthesis of controlled particle size ZIF-67 samples: ZIF-67 with particle size of 2000 nm is synthesised similar to above described method except adding 8 ml 1-methylimidazole. ZIF-67 *with particle size of 50 nm and 200 nm are synthesised as following:* 5.9 g cobalt nitrate hexahydrate and 0.5 g polyvinylpyrrolidone (PVP) were dissolved in a 500 ml methanol. Then 6.65 g of 2-methyl imidazole was mixed in another 500 ml methanol. Then the solution was stirring and slowly added to the metal precursor solution. After a few minutes the solution changed from the pink to purple, which was then left for a day to settle. Clear solution was poured out and the precipitate sample was extracted after several washings by methanol. All the samples were dried at 80 °C oven. The 50 nm ZIF-67 and 200 nm ZIF-67 were prepared with different amounts of TEA (triethylamine) (60 µL and 22.5 µL, respectively).

Composites of ZIF-67/CB were obtained by mixing of CB and ZIF-67 powders in different mass ratios (of CB in 25 wt%, 50 wt%, and 75 wt %) using deionised water dispersion method under sonication, the same method of preparing catalyst ink for electrode preparation. The as-synthesized sample were then used for electrochemical test.

Powder X-ray diffraction patterns (PXRD) were collected by Stoe Stadi-P, Mo–K-alpha. Fourier-transform infrared (FTIR) data was obtained by Bruker ALPHA FTIR Spectrometer (Platinum-ATR) with background correction. X-ray photoemission spectroscopy (XPS, on Al–K-alpha, Thermo Scientific) data and scanning electron microscopy (SEM, on JSM6700, Jeol) measurements were carried out on the samples supported on a carbon tape. The porosity by N_2 and CO_2 adsorption-desorption isotherms were measured at 77 K and 298 K, respectively, on a Quantachrome Autosorb-iQC. All the samples were degassed at 180 ℃ overnight under a dynamic vacuum prior to the actual gas adsorption measurements. The specific surface area was measured from the 77 K N_2 isotherm in a relative pressure range between 0.01 and 0.2, according to the Brunauer–Emmett–Teller (BET) method. The pore volume was obtained from the adsorption volume at relative pressure of 0.95. Thermogravimetric analysis was carried out up to 1000 °C at a heating rate of 5 °C per minute and kept at 1000 °C for 1 h under argon atmosphere, using Setaram, Setsys kit.

All the electrochemical catalytic activity of the samples were reported using a potentiostation (Autolab, Metrohm PGSTAT302N) with a rotating-disk three-electrode (RDE) cell configuration composed of a glassy carbon electrode (GCE) rotating disk with active material as working electrode, and (1 × 1) cm^2 Pt and Ag/AgCl/saturated KCl as counter and reference electrode, respectively. All the measurements were carried out in O_2-saturated alkaline (0.1 M KOH and 1.0 M KOH) electrolyte at room temperature. The catalyst loading was fixed at ~0.28 mg cm^{-2} on a 3 mm diameter (or area of 0.0707 cm^2) glassy carbon electrode (GCE). The catalyst was prepared as follows; 2 mg of sample was dispersed in a total 500 ml solution consisting 482 ml of deionized water plus 18 ml of Nafion (5% solution) under sonication. The sonication was carried out for up to an hour to get uniform catalyst dispersion of ink. Of this 5 ml was micropipetted and dropped on to a GCE followed by drying at <60 ℃ in an oven prior to the electrochemical tests. The cyclic voltammetry (CV) and linear sweep voltammetry (LSV) curves were recorded with a voltage sweeping at 10 mV s^{-1} in the potential range of +0.2 V to +1.0 V in case of OER and in the range of +0.2 V to −0.8 V in case of ORR. OER durability tests by chronoamperometric (*I vs t*) were carried out at a fixed potential of +1.65 V (vs RHE), and the response current was recorded against time. In chronopotentiometry (*V vs t*), the response potential was recorded against time at a fixed current density of 10 mA cm^{-2}. All of the OER and ORR LSV curves were recorded at constant rpm of 1600. All the reported current densities were estimated by normalizing the actual current response to the electrode area of GCE. The following relation is used for potential representation V (vs RHE) = $E_{Ag/AgCl}$ + 0.197 + 0.059 × pH. The overpotential is reported according to the relation; V = V_{RHE} − 1.23 V.

Acknowledgements

Authors are grateful to Prof Zhengxiao Guo and Prof Ivan Parkin.

Keywords: metal-organic frameworks (MOFs) • oxygen evolution reaction (OER) • zeolitic imidazolate frameworks (ZIFs) • electrocatalysts.

[1] S. Dang, Q.-L. Zhu, Q. Xu, Nat. Rev. Mater. 2017, 3, 17075.
[2] W. Yang, X. Li, Y. Li, R. Zhu, H. Pang, Adv. Mater. 2018, 31, 1804740.
[3] K. Shen, L. Zhang, X. Chen, L. Liu, D. Zhang, Y. Han, J. Chen, J. Long, R. Luque, Y. Li, B. Chen, Science. 2018, 359, 206.
[4] X. Xiao, L. Zou, H. Pang, Q. Xu, Chem. Soc. Rev. 2020, 49, 301.
[5] W. Liu, R. Yin, X. Xu, L. Zhang, W. Shi, X. Cao, Adv. Sci. 2019, 6, 1802373.
[6] Z. Xue, Y. Li, Y. Zhang, W. Geng, B. Jia, J. Tang, S. Bao, H.-P. Wang, Y. Fan, Z. Wei, Z. Zhang, Z. Ke, G. Li, C.-Y. Su, Adv. Energy Mater. 2018, 8, 1801564.
[7] S. Gadipelli, Z. Li, Y. Lu, J. Li, J. Guo, N. T. Skipper, P. R. Shearing, D. J. L. Brett, Adv. Sci. 2019, 6, 1901517.

[8] C. Lei, S. Lyu, J. Si, B. Yang, Z. Li, L. Lei, Z. Wen, G. Wu, Y. Hou, ChemCatChem 2019, 11, 5855.
[9] J. Cao, K. Wang, J. Chen, C. Lei, B. Yang, Z. Li, L. Lei, Y. Hou, K. Ostrikov, Nano-Micro Lett. 2019, 11, 1.
[10] J. Cao, C. Lei, J. Yang, X. Cheng, Z. Li, B. Yang, X. Zhang, L. Lei, Y. Hou, K. Ostrikov, J. Mater. Chem. A 2018, 6, 18877.
[11] J. Cao, C. Lei, B. Yang, Z. Li, L. Lei, Y. Hou, X. Feng, Batter. Supercaps 2019, 2, 348.
[12] X. Li, J. Wei, Q. Li, S. Zheng, Y. Xu, P. Du, C. Chen, J. Zhao, H. Xue, Q. Xu, H. Pang, Adv. Funct. Mater. 2018, 28, 1800886.
[13] X. Li, C. Wang, H. Xue, H. Pang, Q. Xu, Coord. Chem. Rev. 2020, 422, 213468.
[14] L. Lei, D. Huang, M. Cheng, R. Deng, S. Chen, Y. Chen, W. Wang, Coord. Chem. Rev. 2020, 418, 213372.
[15] R. Zhu, J. Ding, J. Yang, H. Pang, Q. Xu, Q. Xu, D. Zhang, P. Braunstein, ACS Appl. Mater. Interfaces 2020, 12, 25037.
[16] G. Srinivas, V. Krungleviciute, Z. X. Guo, T. Yildirim, Energy Environ. Sci. 2014, 7, 335.
[17] Y. Bai, G. Zhang, S. Zheng, Q. Li, H. Pang, Q. Xu, Sci. China Mater. 2020, 1.
[18] L. Kong, M. Zhong, W. Shuang, Y. Xu, X.-H. Bu, Chem. Soc. Rev. 2020, 49, 2378.
[19] S. Gadipelli, W. Travis, W. Zhou, Z. Guo, Energy Environ. Sci. 2014, 7, 2232.
[20] J. Teng, M. Chen, Y. Xie, D. Wang, J. J. Jiang, G. Li, H. P. Wang, Y. Fan, Z. W. Wei, C. Y. Su, Chem. Mater. 2018, 30, 6458.
[21] Q. Qian, Y. Li, Y. Liu, L. Yu, G. Zhang, Adv. Mater. 2019, 31, 1901139.
[22] L. Zhuang, L. Ge, H. Liu, Z. Jiang, Y. Jia, Z. Li, D. Yang, R. K. Hocking, M. Li, L. Zhang, X. Wang, X. Yao, Z. Zhu, Angew. Chem. Int. Ed. 2019, 58, 13565.
[23] T. Liu, P. Li, N. Yao, T. Kong, G. Cheng, S. Chen, W. Luo, Adv. Mater. 2019, 31, 1806672.
[24] T. Wen, Y. Zheng, J. Zhang, K. Davey, S. Qiao, Adv. Sci. 2019, 6, 1801920.
[25] N. Y. Huang, J. Q. Shen, Z. M. Ye, W. X. Zhang, P. Q. Liao, X. M. Chen, Chem. Sci. 2019, 10, 9859.
[26] X. Li, X. Yang, H. Xue, H. Pang, Q. Xu, EnergyChem 2020, 2, 100027.
[27] X. L. Wang, L. Z. Dong, M. Qiao, Y. J. Tang, J. Liu, Y. Li, S. L. Li, J. X. Su, Y. Q. Lan, Angew. Chem. Int. Ed. 2018, 57, 9660.
[28] K. Zhou, B. Mousavi, Z. Luo, S. Phatanasri, S. Chaemchuen, F. Verpoort, J. Mater. Chem. A 2017, 5, 952.
[29] W. Chen, Y. Zhang, G. Chen, Y. Zhou, X. Xiang, K. K. Ostrikov, ACS Sustain. Chem. Eng. 2019, 7, 8255.
[30] Z.-F. Huang, J. Song, Y. Du, S. Xi, S. Dou, J. M. V. Nsanzimana, C. Wang, Z. J. Xu, X. Wang, Nat. Energy 2019, 4, 329.
[31] X. Liu, Z. Chang, L. Luo, T. Xu, X. Lei, J. Liu, X. Sun, Chem. Mater. 2014, 26, 1889.
[32] J. Zang, F. Wang, Q. Cheng, G. Wang, L. Ma, C. Chen, L. Yang, Z. Zou, D. Xie, H. Yang, J. Mater. Chem. A 2020, 8, 3686.
[33] M. Rubio-Martinez, C. Avci-Camur, A. W. Thornton, I. Imaz, D. Maspoch, M. R. Hill, Chem. Soc. Rev. 2017, 46, 3453.
[34] F. Hillman, J. M. Zimmerman, S. M. Paek, M. R. A. Hamid, W. T. Lim, H. K. Jeong, J. Mater. Chem. A 2017, 5, 6090.
[35] S. Gadipelli, Z. Li, T. Zhao, Y. Yang, T. Yildirim, Z. Guo, J. Mater. Chem. A 2017, 5, 24686.
[36] K. S. Park, Z. Ni, A. P. Cote, J. Y. Choi, R. Huang, F. J. Uribe-Romo, H. K. Chae, M. O'Keeffe, O. M. Yaghi, Proc. Natl. Acad. Sci. 2006, 103, 10186.
[37] S. Gadipelli, T. Zhao, S. A. Shevlin, Z. Guo, Energy Environ. Sci. 2016, 9, 1661.
[38] Z. Jiang, L. Ge, L. Zhuang, M. Li, Z. Wang, Z. Zhu, ACS Appl. Mater. Interfaces 2019, 11, 44300.
[39] T. Zhao, S. Gadipelli, G. He, M. J. Ward, D. Do, P. Zhang, Z. Guo, ChemSusChem 2018, 11, 1295.
[40] Y. Cheng, Y. Wang, Q. Wang, Z. Liao, Ni. Zhang, Y. Guo, Z. Xiang, J. Mater. Chem. A 2019, 7, 9831.
[41] F.-L. Li, Q. Shao, X. Huang, J.-P. Lang, Angew. Chem. Int. Ed. 2018, 57, 1888.
[42] P. M. Usov, C. Mcdonnell-worth, F. Zhou, D. R. Macfarlane, D. M. D. Alessandro, Electrochim. Acta 2015, 153, 433.
[43] Q. Zha, W. Xu, X. Li, Y. Ni, Dalt. Trans. 2019, 48, 12127.
[44] W. Zheng, M. Liu, L. Y. S. Lee, ACS Catal. 2020, 10, 81.
[45] Y. Liang, J. Wei, Y. X. Hu, X. F. Chen, J. Zhang, X. Y. Zhang, S. P. Jiang, S. W. Tao, H. T. Wang, Nanoscale 2017, 9, 5323.
[46] J. Xu, P. Gao, T. S. Zhao, Energy Environ. Sci. 2012, 5, 5333.
[47] G. Chen, J. Zhang, F. Wang, L. Wang, Z. Liao, E. Zschech, K. Müllen, X. Feng, Chem. – A Eur. J. 2018, 24, 18413.

Entry for the Table of Contents

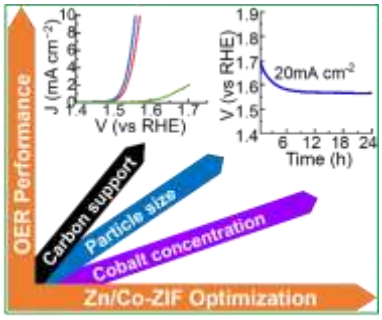

Optimized zeolitic imidazolate frameworks, which can be readily synthesized reproducibly and commercially available, leads to remarkably enhanced electrocatalytic performance in terms of lower overpotential and long-term durability for oxygen evolution reaction (OER).

Institute and/or researcher Twitter usernames: tutelarymoon